DOI: 10.12905/0380.phyton61-2021-0031 Published online 2 Dec 2021

Expression of genes encoding carbohydrate-metabolic enzymes during taproot development in sugar beet (*Beta vulgaris* subsp. *vulgaris*)

Alexandra Jammer[1], Alfonso Albacete[1,$], Britta Schulz[2], Wolfgang Koch[2], Fridtjof Weltmeier[2], Eric van der Graaff[1,3,§] & Thomas Roitsch[3,4,5]

with 5 figures and 4 tables

Key words: *Beta vulgaris* subsp. *vulgaris*; assimilate partitioning; carbohydrate metabolism; developmental regulation; taproot development; sucrose accumulation.

Summary

Jammer A., Albacete A., Schulz B., Koch W., Weltmeier F., van der Graaff E. & Roitsch T. 2021. Expression of genes encoding carbohydrate-metabolic enzymes during taproot development in sugar beet (*Beta vulgaris* subsp. *vulgaris*). – Phyton (Horn, Austria) 61: 31–50, with 5 figures and 4 tables.*

In sugar beet (*Beta vulgaris* subsp. *vulgaris*, *Chenopodiaceae*), sucrose is stored in a taproot developed by a genus-specific type of anomalous secondary thickening from supernumerary cambial rings. In a previous study (Jammer & al. 2020), we showed that the transition from primary root development to the formation of the sucrose-storing taproot is accompanied by a clear shift in physiological signatures: characteristic changes in the activities of several key enzymes of carbohydrate metabolism were associated with the onset of taproot development and sucrose storage, resulting in three distinct physiological stages (prestorage, transition, secondary growth and sucrose storage). In order to investigate the regulatory mechanisms behind these changes in enzyme activities, we performed a microarray expression analysis for the genes encoding the respective carbohydrate-metabolic enzymes. The data obtained from the microarray were validated for selected transcripts by semi-quantitative reverse transcription PCR. A high level of similarity between the developmental changes in transcript levels and enzyme activities at the transition stage suggests that the majority of the respective enzymes are predominantly regulated on the transcriptional level during the early stages of taproot development.

1. Introduction

Sugar beet is a cultivar of *Beta vulgaris* L. subsp. *vulgaris* (*Chenopodiaceae*), and one of two crop species cultivated for the production of sucrose. As a biennial plant, sugar beet forms a storage root, also referred to as the taproot or beet-root, composed of root and hypocotyl tissues. In this taproot, the plant accumulates large amounts of sucrose in the first growing season, which serves as an energy source for bolting and flowering following cold vernalization in the second year (Milford 2006).

The taproots in the genus *Beta* arise from an anomalous type of secondary root thickening involving the formation of supernumerary cambial rings (Artschwager 1926, Zamski & Azenkot 1981, Elliott & Weston 1993, Krumbiegel 1998, Getz 2000, Milford 2006, Fasahat & al. 2018). In the mature beet-root, zones of vascular tissues and zones

[1]) Institute of Biology, University of Graz, NAWI Graz, Schubertstraße 51, 8010 Graz, Austria; corresponding author: A. Jammer (e-mail: alexandra.jammer@uni-graz.at)

[2]) KWS SAAT SE & Co. KGaA, Postfach 1363, 37554 Einbeck, Germany

[3]) Department of Plant and Environmental Sciences, Copenhagen Plant Science Centre, University of Copenhagen, Højbakkegård Allé 13, 2630 Taastrup, Denmark; corresponding author: T. Roitsch (e-mail: roitsch@plen.ku.dk)

[4]) Department of Adaptive Biotechnologies, Global Change Research Institute CAS, Bělidla 986/4a, 60300 Brno, Czech Republic

[5]) Department of Crop Sciences, UFT Tulln, University of Natural Resources and Life Sciences (BOKU), 3430 Tulln, Austria

[$]) Present address: Department of Plant Production and Agrotechnology, Institute for Agri-Food Research and Development of Murcia (IMIDA), C/ Mayor s/n, 30150 La Alberca, Murcia, Spain

[§]) Present address: Koppert Cress B.V., De Poel 1, 2681 MB Monster, The Netherlands

*) Printed volume published ## ### ####

of parenchymatic tissues can be found in an alternating pattern (Elliott & Weston 1993), and sucrose is stored in the vacuoles of the parenchyma cells between and within the vascular rings (Giaquinta 1979, Leigh & al. 1979).

The developing taproots are sink organs that are dependent on the import of carbohydrates from the photosynthetically active source leaves via the phloem pathway, mostly in the form of sucrose (Slewinski & Braun 2010, Wang & Ruan 2016, Li & al. 2017). Due to their anomalous growth characteristics, *Beta* roots represent a special type of sink: from a very early developmental stage onwards, they are consuming sinks using sucrose as an energy source (actively dividing meristems, expanding cells) and storage sinks (sucrose-storing cells) at the same time (Wyse 1979, Getz 2000). Therefore, a fine-tuned regulatory network is required to ensure the distribution of the sucrose allocated to the taproot between the various processes, namely energy release through respiration, macromolecule biosynthesis, sugar signaling, and sucrose storage.

Beet sugar yield, the central parameter of interest for breeders and producers, is a product of two traits that are negatively correlated with each other: sugar content and taproot biomass (Pack 1927, Artschwager 1930, Doney & al. 1981, Bosemark 2006, Stich & al. 2008, Fasahat & al. 2021). Breeding efforts to improve relative sugar content are known to reduce beet yield, and vice versa (Artschwager 1930, Powers 1956, Bergen 1967, Oldemeyer 1975, Fasahat & al. 2021), suggesting that common regulatory mechanisms may be involved in the development of both traits (Doney & al. 1981, Milford 2006).

Despite the agronomic importance of sugar beet, there is still surprisingly little knowledge about the factors that determine sugar yield through the regulation of taproot biomass and sugar content, and the factors responsible for the negative coupling of the two traits have remained elusive (Fasahat & al. 2021). Especially the initial stages of taproot development have been poorly investigated, although several studies published over many decades indicate that the decisive events that determine final beet yield and sugar content take place at this stage (Artschwager 1926, Doney 1979, Giaquinta 1979, Elliott & Weston 1993, Getz 2000, Hoffmann & al. 2005). Still, the studies that aimed at identifying regulators of sucrose content and root yield were mostly focused on mature beets or started at developmental stages when secondary growth had already begun (e.g., Bellin & al. 2002, Herwig & al. 2002, Bellin & al. 2007, Zhang & al. 2017).

In a previous study (Jammer & al. 2020), we physiologically characterized the first 80 days of sugar beet taproot development, with a focus on the developmental regulation of the key enzymes of carbohydrate metabolism in the taproots during that period. Three distinct developmental stages of the (tap)roots – primary growth stage, transition stage, and secondary growth and sucrose storage stage – were identified, which were characterized by distinct physiological signatures. The observed activity patterns for fourteen key enzymes of carbohydrate metabolism, as well as the patterns of soluble carbohydrate and hexose-phosphate levels, were very robust and largely independent of the environmental conditions (for a summary, see Table 1). The prestorage stage was characterized by high invertase activities and a high hexose-to-sucrose ratio, while the later stages were characterized by a broader spectrum of highly active enzymes and a large increase in sucrose content. During the transition stage, changes could be observed for most of the parameters that were analyzed. With this study, we confirmed that the metabolic switch to secondary growth and sucrose storage occurs at a very early developmental stage.

In the present work, we complemented the data from the previous work (Jammer & al. 2020) with gene expression data. Our objective was to investigate to which extent the developmental patterns in enzyme activities observed in our previous study were a consequence of regulation on the transcriptional level. We performed a microarray analysis on taproot samples obtained over the first 80 days of sugar beet development. After mapping the oligo probes on the array against the RefBeet1.2 database, we extracted the expression data for all sequences in the sugar beet genome encoding the same set of carbohydrate-metabolic enzymes we addressed in our previous study (Jammer & al. 2020). In a final step, the array data for selected transcripts were validated by semi-quantitative reverse transcription PCR (semi-qRT PCR). Taken together, the physiological dataset (Jammer & al. 2020) and the gene expression dataset provide further insight into the mechanisms that regulate carbohydrate metabolism during the early stages of taproot development.

2. Materials and methods

Plant material and growth conditions. Sugar beet seeds (*Beta vulgaris* L. subsp. *vulgaris*, *Chenopodiaceae*) were supplied by KWS SAAT SE & Co. KGaA (Einbeck, Germany). The plants were grown in the greenhouse under semi-controlled growth conditions, at 20 °C to 24 °C achieved by additional heating during colder outside temperatures, and a 16 h/8 h day/night cycle by supplementary illumination (Plug and GrowTM 200 W 6400 K fluorescent lamps; Trade Hydro, Cleckheaton, UK), resulting in photosynthetically active radiation of

Table 1. Phases of early-stage sugar beet taproot development and their physiological key characteristics (as previously described by Jammer & al. 2020).

Abbreviations: Ald = aldolase; das = days after sowing; FK = fructokinase; G6PDH = glucose-6-phosphate dehydrogenase; PFK = phosphofructokinase; PGI = phosphoglucoisomerase; PGM = phosphoglucomutase; SuSy = sucrose synthase; UGPase = UDP-glucose pyrophosphorylase.

stage	**prestorage**	**transition**	**secondary growth and sucrose storage**
timespan*	up to 30 das	30 – 60 das	60 das onwards
main processes	primary root development	onset of secondary growth and sucrose storage	taproot development (secondary growth and sucrose storage)
regulation of enzyme activities	high invertase activities	down-regulation of invertases; up-regulation of SuSy, PFK, PGI, PGM, G6PDH, and UGPase; transient up-regulation of Ald and FK	high activities of SuSy, PFK, PGI, PGM, G6PDH, and UGPase
soluble carbohydrates	high hexose-to-sucrose ratio	levels of glucose, fructose, and sucrose increase; hexose-to-sucrose ratio decreases	levels of glucose and fructose stabilize; levels of sucrose strongly increase; low hexose-to-sucrose ratio
hexose phosphates	low levels of G6P, F6P, and G1P	hexose phosphate levels increase	hexose phosphate levels reach a plateau or decrease slightly

*) Timespans as observed in a series of six greenhouse experiments performed by Jammer & al. (2020); the timing of the phase transition depends on the growth conditions.

Table 2. Overview of protein and DNA sequences for carbohydrate-metabolic enzymes in sugar beet.

Protein function	**RefBeet 1.2 protein ID**	**Gene annotation(s) according to NCBI Blast**
ADP-glucose pyrophosphorylase	Bv_004380_znjm	XM_010668476/XM_010668477; predicted: *Beta vulgaris* subsp. *vulgaris* glucose-1-phosphate adenylyltransferase large subunit 3, chloroplastic/amyloplastic (LOC104883901), two transcript variants
	Bv1_007110_kmky	NM_001303063; *Beta vulgaris* subsp. *vulgaris* glucose-1-phosphate adenylyltransferase large subunit, chloroplastic/amyloplastic (LOC104889614)
		X78900; *B.vulgaris* agpS1 mRNA for ADP-glucose pyrophosphorylase
		XM_019251187; predicted: *Beta vulgaris* subsp. *vulgaris* glucose-1-phosphate adenylyltransferase large subunit, chloroplastic/amyloplastic (LOC104889614), transcript variant X1, mRNA
	Bv3_059420_fjac*	XM_019248653; predicted: *Beta vulgaris* subsp. *vulgaris* inactive glucose-1-phosphate adenylyltransferase small subunit 2, chloroplastic (LOC104889127), mRNA
	Bv9_206950_yrsx	XM_010691051; predicted: *Beta vulgaris* subsp. *vulgaris* glucose-1-phosphate adenylyltransferase small subunit, chloroplastic/amyloplastic (LOC104903071)
		X78899; *B. vulgaris* agpB1 mRNA for ADP-glucose pyrophosphorylase
	Bv9_217200_yktd	XM_010692547; predicted: *Beta vulgaris* subsp. *vu*lgaris glucose-1-phosphate adenylyltransferase large subunit 1 (LOC104904329)
Aldolase	Bv4_078150_cgxu	XM_010676043/XM_010676044/XM_010676045; predicted: *Beta vulgaris* subsp. *vulgaris* fructose-bisphosphate aldolase 3, chloroplastic (LOC104890526), three transcript variants
		XM_010685482; predicted: *Beta vulgaris* subsp. *vulgaris* fructose-bisphosphate aldolase 3, chloroplastic (LOC104898399)

*) not on the array used for this study

Table 2 (continued). Overview of protein and DNA sequences for carbohydrate-metabolic enzymes in sugar beet.

Protein function	RefBeet 1.2 protein ID	Gene annotation(s) according to NCBI Blast
Aldolase (continued)	Bv4_091040_cyuu	XM_010677812; predicted: *Beta vulgaris* subsp. *vulgaris* fructose-bisphosphate aldolase 5, cytosolic (LOC104892005)
	Bv6_129880_fskg	XM_010681546; predicted: *Beta vulgaris* subsp. *vulgaris* fructose-bisphosphate aldolase 1, chloroplastic (LOC104895124)
		XM_010692461; predicted: *Beta vulgaris* subsp. *vulgaris* fructose-bisphosphate aldolase 1, chloroplastic (LOC104904258)
		AF173645; *Beta vulgaris* clone ALDP109REV fructose-1, 6-bisphosphate aldolase (Aldch1) gene, partial sequence
		XM_019247968; predicted: *Beta vulgaris* subsp. *vulgaris* fructose-bisphosphate aldolase 1, chloroplastic-like (LOC104887224)
	Bv7_159930_ugdi	XM_010676043/XM_010676044/XM_010676045; predicted: *Beta vulgaris* subsp. *vulgaris* fructose-bisphosphate aldolase 3, chloroplastic (LOC104890526), three transcript variants
		XM_010685482; predicted: *Beta vulgaris* subsp. *vulgaris* fructose-bisphosphate aldolase 3, chloroplastic (LOC104898399)
	Bv7_160160_nqkh	XM_010685561; predicted: *Beta vulgaris* subsp. *vulgaris* fructose-bisphosphate aldolase, cytoplasmic isozyme (LOC104898474)
		AF173646; *Beta vulgaris* clone ALD109UNI cytosolic fructose 1,6-bisphosphate aldolase (Aldcyt) gene, partial sequence
	Bv9_216490_wffm*	XM_010692461; predicted: *Beta vulgaris* subsp. *vulgaris* fructose-bisphosphate aldolase 1, chloroplastic (LOC104904258)
		XM_010681546; predicted: *Beta vulgaris* subsp. *vulgaris* fructose-bisphosphate aldolase 1, chloroplastic (LOC104895124)
		AF173645; *Beta vulgaris* clone ALDP109REV fructose-1, 6-bisphosphate aldolase (Aldch1) gene, partial sequence
		XM_019247968; predicted: *Beta vulgaris* subsp. *vulgaris* fructose-bisphosphate aldolase 1, chloroplastic-like (LOC104887224)
Cell wall-bound invertase	Bv2_034520_mthe	XM_010671083; predicted: *Beta vulgaris* subsp. *vulgaris* beta-fructofuranosidase, insoluble isoenzyme CWINV3 (BIN46), mRNA
		AJ422053; *Beta vulgaris* mRNA for exocellular acid invertase 2 (exinv2 gene)
		AJ277969; *Beta vulgaris* cwinit gene for cell wall invertase, exons 1–7
		X81797; *B.vulgaris* BIN46 mRNA for extracellular invertase
	Bv7_159240_owqs	XM_010685400; predicted: *Beta vulgaris* subsp. *vulgaris* beta-fructofuranosidase, insoluble isoenzyme 1 (LOC104898340)
	Bv7_170570_jfzr*	XM_010687078; predicted: *Beta vulgaris* subsp. *vulgaris* beta-fructofuranosidase, cell wall isozyme-like (LOC104899808)
	Bv7_170580_aiyc	XM_010687080; predicted: *Beta vulgaris* subsp. *vulgaris* fructan 6-exohydrolase (LOC104899809), transcript variant X2
		AJ277458; *Beta vulgaris* partial cwiwit gene for cell wall invertase
		XM_010687079; predicted: *Beta vulgaris* subsp. *vulgaris* fructan 6-exohydrolase (LOC104899809), transcript variant X1
		AJ422052; *Beta vulgaris* mRNA for exocellular acid invertase 1 (exinv1 gene) [= BIN35]
		X81795; *B.vulgaris* BIN35 mRNA for extracellular invertase
		AJ278531; *Beta vulgaris* partial mRNA for invertase (cwi1 gene)

*) not on the array used for this study

Table 2 (continued). Overview of protein and DNA sequences for carbohydrate-metabolic enzymes in sugar beet.

Protein function	RefBeet 1.2 protein ID	Gene annotation(s) according to NCBI Blast
Cytoplasmic invertase	Bv_007210_orig	XM_010668887; predicted: *Beta vulgaris* subsp. *vulgaris* alkaline/neutral invertase A, mitochondrial (LOC104884264)
		XM_010687767; predicted: *Beta vulgaris* subsp. *vulgaris* neutral/alkaline invertase 3, chloroplastic (LOC104900355)
		AJ422050; *Beta vulgaris* mRNA for neutral invertase (ninv gene)
	Bv1_001200_oroi	XM_010681123; predicted: *Beta vulgaris* subsp. *vulgaris* probable alkaline/neutral invertase D (LOC104894771)
	Bv1_002810_zahj*	XM_010675648; predicted: Beta vulgaris subsp. vulgaris probable alkaline/neutral invertase F (LOC104890239)
	Bv1_016180_pewc	XM_010693556/XM_010693557; predicted: *Beta vulgaris* subsp. *vulgaris* probable alkaline/neutral invertase B (LOC104905111), two transcript variants
	Bv4_080050_ocda	XM_010676257; predicted: *Beta vulgaris* subsp. *vulgaris* alkaline/neutral invertase A, mitochondrial (LOC104890680)
		AJ422050; *Beta vulgaris* mRNA for neutral invertase (ninv gene)
	Bv9_214690_sjah	XM_010692146/XM_010692147/XM_010692148; predicted: *Beta vulgaris* subsp. *vulgaris* probable alkaline/neutral invertase B (LOC104903987), three transcript variants
Fructokinase	Bv2_027840_oqrd	XM_010695633; predicted*: Beta vulgaris* subsp. *vulgaris* probable fructokinase-6, chloroplastic (LOC104906815)
	Bv3_057460_dyyp	XM_010673922; predicted: *Beta vulgaris* subsp. *vulgaris* probable fructokinase-4 (LOC104888823)
		BVU37838; *Beta vulgaris* fructokinase mRNA, complete cds
	Bv3_066020_xjni	XM_010695140; predicted: *Beta vulgaris* subsp. *vu*lgaris probable fructokinase-7 (LOC104906399)
	Bv5_120550_omcz	XM_010680890; predicted: *Beta vulgaris* subsp. *vulgaris* fructokinase-1 (LOC104894611)
	Bv6_136290_jzyk	XM_010682360/XM_019250192; predicted: *Beta vulgaris* subsp. *vulgaris* fructokinase-like 2, chloroplastic (LOC104895770), two transcript variants
	Bv7_178860_gedd	XM_010697961; predicted: *Beta vulgaris* subsp. *vulgaris* probable fructokinase-5 (LOC104908806)
	Bv8_182100_hsoh	XM_010688048; *Beta vulgaris* subsp. *vulgaris* fructokinase-like 1, chloroplastic (LOC104900588)
Glucose-6-phosphate dehydrogenase	Bv1_011600_gazr	XM_010682427; predicted: *Beta vulgaris* subsp. *vulgaris* glucose-6-phosphate 1-dehydrogenase, cytoplasmic (LOC104895811)
	Bv4_079860_qtuq	XM_010676236/ XM_010676237; predicted: *Beta vulgaris* subsp. *vulgaris* glucose-6-phosphate 1-dehydrogenase 4, chloroplastic (LOC104890663), two transcript variants
	Bv6_150380_hjur	XM_010684411; predicted: *Beta vulgaris* subsp. *vulgaris* glucose-6-phosphate 1-dehydrogenase, chloroplastic (LOC104897526)
	Bv9_206300_yiew	AF173650; *Beta vulgaris* clone GPD109UNI glucose-6-phosphate dehydrogenase (Gpd) gene, partial sequence
		XM_010690958; predicted*: Beta vulgaris* subsp. *vulgaris* glucose-6-phosphate 1-dehydrogenase, chloroplastic (LOC104902995)
Hexokinase	Bv4_073320_tcog	XM_010675406; predicted: *Beta vulgaris* subsp. *vulgaris* hexokinase-3 (LOC104890049)
	Bv5_124820_xpum	XM_010697123; predicted: *Beta vulgaris* subsp. *vu*lgaris hexokinase-2, chloroplastic (LOC104908065)

*) not on the array used for this study

Table 2 (continued). Overview of protein and DNA sequences for carbohydrate-metabolic enzymes in sugar beet.

Protein function	RefBeet 1.2 protein ID	Gene annotation(s) according to NCBI Blast
Hexokinase (continued)	Bv8_197580_aaut	XM_010690039; predicted: *Beta vulgaris* subsp. *vulgaris* hexokinase-1 (LOC104902309)
	Bv9_224670_aurc	XM_010667582; predicted: *Beta vulgaris* subsp. *vulgaris* hexokinase-1 (LOC104883129)
	Bv9_224680_aote	XM_010667583/XM_010667584; predicted: *Beta vulgaris* subsp. *vulgaris* hexokinase-1 (LOC104883130), two transcript variants
Invertase inhibitor	Bv5_105730_mpgs*	XM_010678914; predicted: *Beta vulgaris* subsp. *vulgaris* putative invertase inhibitor (LOC104892892)
	Bv6_139440_ueqi	XM_010682800; predicted: *Beta vulgaris* subsp. *vulgaris* 21 kDa protein (LOC104896099); 38 % identity on the protein level with NM_102169.3 (*A. thaliana* AT1G23205); putative plant invertase/pectin methylesterase inhibitor superfamily protein
	Bv8_190760_taam*	XM_010689248; predicted: *Beta vulgaris* subsp. *vulgaris* putative invertase inhibitor (LOC104901655)
	Bv8_190770_hutw*	XM_010689483; predicted: *Beta vulgaris* subsp. *vulgaris* putative invertase inhibitor (LOC104901857)
Phospho-fructokinase	Bv2_046600_nsyu	XM_010694928; predicted: *Beta vulgaris* subsp. *vulgaris* ATP-dependent 6-phosphofructokinase 5, chloroplastic (LOC104906202)
	Bv6_138960_rsmr	XM_010682742; predicted: *Beta vulgaris* subsp. *vulgaris* ATP-dependent 6-phosphofructokinase 5, chloroplastic (LOC104896058)
	Bv6_153060_mqdn	XM_010684772; predicted: *Beta vulgaris* subsp. *vulgaris* ATP-dependent 6-phosphofructokinase 2 (LOC104897825)
	Bv8_185430_exsc	XM_010688467; predicted: *Beta vulgaris* subsp. *vulgaris* pyrophosphate--fructose 6-phosphate 1-phosphotransferase subunit beta (LOC104900934)
	Bv8_197870_dtpx	XM_010690076; predicted: *Beta vulgaris* subsp. v*ulgaris* ATP-dependent 6-phosphofructokinase 6 (LOC104902340)
	Bv9_212010_mhum	XM_010691839; predicted: *Beta vulgaris* subsp. *vulgaris* ATP-dependent 6-phosphofructokinase 3 (LOC104903729)
	Bv2_032880_zzcx*	XM_010670508; predicted: *Beta vulgaris* subsp. *vulgaris* ATP-dependent 6-phosphofructokinase 6 (LOC104885917)
Phosphoglucoisomerase	Bv1_007880_snqy	XM_010677045; predicted: *Beta vulgaris* subsp. *vulgaris* glucose-6-phosphate isomerase 1, chloroplastic (LOC104891360)
	Bv5_108180_qtni	XM_010679206; predicted*: Beta vulgaris* subsp. *vulgaris* glucose-6-phosphate isomerase, cytosolic (LOC104893126)
		AF295651; *Beta vulgaris* cytosolic phosphoglucoisomerase (pgi) mRNA, partial cds
		XM_010670886; predicted: *Beta vulgaris* subsp. *vulgaris* glucose-6-phosphate isomerase-like (LOC104886433)
Phosphoglucomutase	Bv3_066000_riyk	XM_010695137; predicted: *Beta vulgaris* subsp. *vulgaris* phosphoglucomutase, chloroplastic (LOC104906396)
	Bv6_144320_unms	XM_010683613; predicted: *Beta vulgaris* subsp. *vulgaris* phosphoglucomutase, cytoplasmic (LOC104896820)
		AF295652; *Beta vulgaris* phosphoglucomutase (pgm) gene, partial cds
Sucrose-phosphate synthase	Bv8_193450_doak	XM_010698229; predicted: *Beta vulgaris* subsp. *vulgaris* sucrose-phosphate synthase (LOC104909043),
	Bv2_030670_mgoq	NM_001303068; *Beta vulgaris* subsp. *vulgaris* probable sucrose-phosphate synthase (SBSPS1)
		X81975; *B. vulgaris* mRNA for sucrose 6-phosphate synthase

*) not on the array used for this study

Table 2 (continued). Overview of protein and DNA sequences for carbohydrate-metabolic enzymes in sugar beet.

Protein function	RefBeet 1.2 protein ID	Gene annotation(s) according to NCBI Blast
Sucrose synthase	Bv4_084720_myet	XM_019249069/XM_010676934/XM_010676936; predicted: *Beta vulgaris* subsp. *vulgaris* sucrose synthase 7 (LOC104891266); three transcript variants
	Bv7_163460_jmqz	XM_010686041; predicted: *Beta vulgaris* subsp. *vulgaris* sucrose synthase (SBSS1)
		AF273253; *Beta vulgaris* sucrose synthase gene, complete cds
		EF660856; *Beta vulgaris* cultivar VDH66156 sucrose synthase 1 (SBSS1) mRNA, complete cds
		X81974; *B.vulgaris* mRNA for sucrose synthase
	Bv7_173620_ffuo*	XM_010687427; predicted: *Beta vulgaris* subsp. *vulgaris* sucrose synthase-like (LOC104900089)
	Bv8_190960_nnjy	XM_019251347/XM_019251348/XM_019251349; predicted: *Beta vulgaris* subsp. *vulgaris* sucrose synthase (LOC104901675), three transcript variants
UDP-glucose pyrophosphorylase	Bv2_045760_wmnk	XM_010694775; predicted: *Beta vulgaris* subsp. *vulgaris* hypothetical protein (LOC104906066) (UTP-glucose-1-phosphate uridylyltransferase 3, chloroplastic
	Bv4_096640_ydmd	XM_010696669; predicted: *Beta vulgaris* subsp. *vulgaris* UTP-glucose-1-phosphate uridylyltransferase (LOC104907700)
Vacuolar invertase	Bv3_056080_iafj	XM_010673724; predicted: *Beta vulgaris* subsp. *vulgaris* beta-fructofuranosidase, soluble isoenzyme I (LOC104888690)
		AJ277456; *Beta vulgaris* partial vi2 gene for beta-fructofuranosidase
		AJ277457; *Beta vulgaris* partial mRNA for beta-fructofuranosidase (vi2 gene)
	Bv5_097930_juac	XM_010677872; predicted: *Beta vulgaris* subsp. *vulg*aris acid beta-fructofuranosidase (BIN44), transcript variant X1 [*Beta vulgaris* vi1 gene for beta-fructofuranosidase]
		AJ277455; *Beta vulgaris* vi1 gene for beta-fructofuranosidase
		XM_010677873; *Beta vulgaris* subsp. *vulgaris* acid beta-fructofuranosidase (BIN44), transcript variant X2
		AJ422051; *Beta vulgaris* mRNA for acid vacuolar invertase (vacinv gene)
		X81796; *B.vulgaris* BIN44 mRNA for intracellular invertase

*) not on the array used for this study

at least 75 µmol photons m^{-2} s^{-1}. The plants were grown in soil (Naturahum; Gramoflor, Vechta, Germany) in containers of different sizes (depending on sampling time point). The taproots were dug from the soil at seven sampling time points (10, 15, 20, 30, 40, 60, and 80 days after sowing; das) and washed with tap water. Pooled samples of at least 15 individuals per time point were frozen in liquid nitrogen. The material was ground in liquid nitrogen, with 0.1 % polyvinyl-polypyrrolidone to bind phenolics, and stored at –80 °C until further use. The material used for this work corresponds to experiment A4-sp in our previous study (Jammer & al. 2020).

RNA isolation. Two independent total RNA extracts were prepared from the ground plant material using the RNeasy Plant Mini Kit (QIAGEN, Hilden, Germany) according to the manufacturer's instructions. RNA quality and content were determined on agarose gels and using a Nanodrop photometer.

Microarray analysis. Microarray hybridization and analysis were performed as previously described by Weltmeier & al. (2011). Two independent hybridizations each were performed for the two independent RNA extracts for each sampling time point. To obtain expression values for current sugar beet gene models, the oligo probe sequences present on the array were mapped against gene model sequences using RefBeet1.2 (for the link to the website, see 'Online resources' below). The transcript datasets for all genes annotated or predicted to encode the proteins of interest were extracted from the array data (for a list of accession numbers and annotations, see Table 2): vacuolar, cytoplasmic and cell wall-bound invertases (vacInv, cytInv, cwInv), invertase inhibitor proteins (InvInh), sucrose synthases (SuSy), hexokinases (HXK), fructokinases

(FK), uridine-5'-diphosphoglucose pyrophosphorylases (UGPase), phosphoglucoisomerases (PGI), phosphoglucomutases (PGM), fructose-1,6-bisphosphate aldolases (Ald), phosphofructokinases (PFK), glucose-6-phosphate dehydrogenases (G6P-DH), adenosine-5'-diphosphoglucose pyrophosphorylases (AGPase), and sucrose-phosphate synthases (SPS). The signal intensities of all probe sets corresponding to a given gene were summarized by calculating Tukey's Biweight Mean. Means were then calculated for each time point for each of the analyzed transcripts from the expression values obtained from the hybridizations with the two RNA extracts (absolute signal intensities and log2 ratios).

Semi-qRT PCR validation of microarray data. For selected sequences, the array data were validated by semi-quantitative reverse transcription PCR (semi-qRT PCR). Five genes that showed different expression levels and stable expression (log2 ratio < ± 0.4) were selected as control genes for normalization (see Table 3). Furthermore, twelve genes encoding carbohydrate-metabolic enzymes were selected from the array for semi-qRT PCR validation. Primers were designed for the target sequences, and the PCR conditions (annealing temperature, number of PCR cycles) were individually adjusted for each primer pair (Table 3) using cDNA from a pooled sugar beet taproot mRNA sample as a template. To confirm the identity of the amplicons, they were cloned into the pJET1.2/blunt vector and transformed into *E. coli*, and the inserts of the isolated recombinant plasmids were subsequently analyzed by DNA sequencing. The linearity of PCR amplification was proven for selected genes at the optimal number of PCR cycles by using a twofold cDNA dilution series (up to 64fold) as templates (Fig. 1). Two independent batches of cDNA were then generated from the two independent batches of total RNA extracts prepared for the microarray analysis. Within each cDNA batch, the samples were normalized for cDNA content based on the mean gray values determined for the bands obtained with each control primer pair and time point. The normalized cDNA samples were used as templates for the PCRs with specific primer pairs for the control genes and the genes of interest. A normalization factor was calculated for each time point from the gray values obtained from the control genes in order to eliminate the remaining variations of cDNA content between the samples. The results for each gene of interest were expressed as means calculated from the log2 ratios of the gray values obtained from two independent sets of PCRs each performed on the two independent batches of cDNA, using expression levels at 10 das as a common reference.

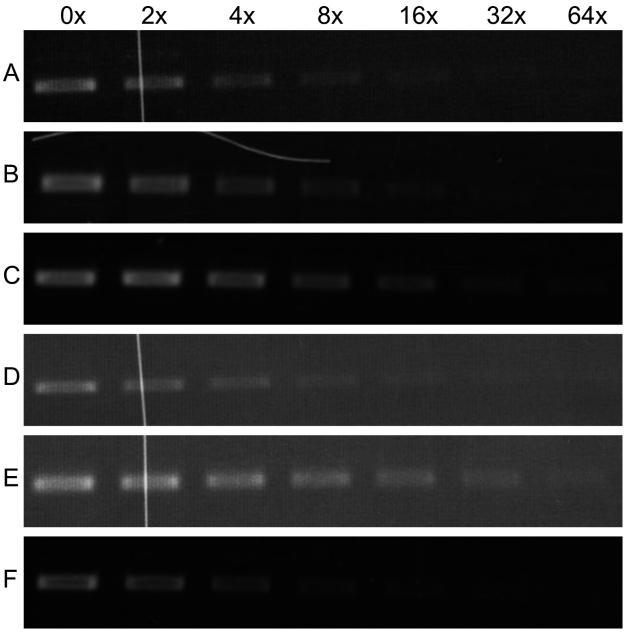

Fig. 1. Test for linearity of semi-qRT PCR amplification. A twofold cDNA dilution series (up to 64fold) was used as templates for amplification at the optimal number of PCR cycles. [A] *Bv3_064110_shhh* (reference gene; 27 cycles, annealing at 68 °C). – [B] *Bv1_000560_nkif* (reference gene; 26 cycles, annealing at 62 °C). – [C] *Bv_004630_emyw* (reference gene; 26 cycles, annealing at 58 °C). – [D] *Bv6_128240_jacf* (reference gene; 25 cycles, annealing at 62 °C). – [E] *Bv1_004960_isam/Bv_011660_mrfn* (reference gene; 25 cycles, annealing at 65 °C). – [F] *Bv3_057460_dyyp* (encodes a fructokinase; 22 cycles, annealing at 65 °C).

Statistical evaluation. The data were analyzed for statistical significance with the unpaired Student's t-test for unequal variances (Welch's t-test) for the significance levels 0.05, 0.01, and 0.001.

Online resources. RefBeet1.2: http://bvseq.boku.ac.at/Genome/Download/RefBeet-1.2/BeetSet-2.genes. 1408.mrna; NCBI Blast: https://blast.ncbi.nlm.nih.gov/Blast.cgi.

3. Results

To analyze the expression of the genes encoding fourteen carbohydrate-metabolic enzymes in developing sugar beet taproots, aiming to complement the physiological data from our previous study (Jammer & al. 2020), a time-course experiment was carried out under semi-standardized conditions. Plant material was sampled at seven time points over 80 days after sowing (das) and used for microarray expression analysis.

3.1. Microarray analysis

For the enzymes and inhibitor proteins of interest – cwInv, cytInv, vacInv, InvInh, SuSy, HXK, FK,

Table 3. Transcripts selected for semi-quantitative RT-PCR validation of microarray data, primer sequences for amplification, PCR conditions, and amplicon sizes.

Category	RefBeet1.2 protein ID	gene annotation according to NCBI Blast	PCR primers (5' – 3')	annealing temperature, number of PCR cycles, amplicon size
Reference gene	Bv3_064110_shhh	XM_010674905; predicted: probable protein-S-acyl-transferase 4 (*Beta vulgaris* subsp. *vulgaris)*	forward: TGAACGAATCCAC CCGTCG reverse: TGATCGAGCCTGG GTTCTC	68 °C 27 cycles 327 bp
	Bv1_000560_nkif	XM_010674842/ XM_01067488; predicted: 1-phosphatidylinositol 3-phosphate 5-kinase FAB1D, 2 transcript variants (*Beta vulgaris* subsp. *vulgaris)*	forward: ATCGGAGTCATGG ATTATTCTC reverse: GGTCAAGAAGTGC GTATCCA	62 °C 26 cycles 222 bp
	Bv_004630_emyw	XM_010668516/ XM_01066851; predicted: vacuolar protein sorting-associated protein 29, 2 transcript variants (*Beta vulgaris* subsp. *vulgaris)*	forward: ACAGCAGCATCAC CTATGAC reverse: TCACCGTCGCTCT GTCTCA	58 °C 26 cycles 214 bp
	Bv6_128240_jacf	XM_010681348; predicted: pentatricopeptide repeat-containing protein At5g67570, chloroplastic (*Beta vulgaris* subsp. *vulgaris)*	forward: CTGTCTCTGCTAT AGTTTACG reverse: GAGTTCTTGCATG AGATCATAA	62 °C 24 cycles 238 bp
	Bv1_004960_isam/ Bv_011660_mrfn	NM_001303085; V-type proton ATPase 16 kDa proteolipid subunit (*Beta vulgaris* subsp. *vulgaris)*	forward: TGGCCATCGGTAT TGTCGG reverse: GTGGCAATGGAA AAACAAATGT	65 °C 25 cycles 210 bp
Aldolase	Bv4_078150_cgxu	XM_010676043/ XM_010676044/ XM_010676045; predicted: fructose-bisphosphate aldo-lase 3, chloroplastic, 3 transcript variants (*Beta vulgaris* subsp. *vulgaris)*	forward: ACGCAACTTGTGG GAAGAGA reverse: AGGCAAAGAAAC CAAACCCTT	65 °C 27 cycles 239 bp
Cell wall-bound invertase	Bv7_170580_aiyc	AJ422052; exocellular acid invertase 1 (exinv1 gene) (*Beta vulgaris*)	forward: GAAACATGTTCT CAAAAATAGCT reverse: ATGTCATCTTCCA CACTCGAA	58 °C 26 cycles 231 bp
Cytoplasmic invertase	Bv1_001200_oroi	XM_010681123; predicted: probable alkaline/neutral invertase D (*Beta vulgaris* subsp. *vulgaris)*	forward: TTCTCATACGTCG ATCTCTGA reverse: GAAGCATGGTCAT AAGCAGC	62 °C 24 cycles 324 bp

Table 3 (continued). Sequences for semi-quantitative RT-PCR validation of microarray data, primer sequences for amplification, PCR conditions, and amplicon sizes.

Category	RefBeet1.2 protein ID	gene annotation according to NCBI Blast	PCR primers (5' – 3')	annealing temperature, number of PCR cycles, amplicon size
Fructokinase	Bv3_057460_dyyp	XM_010673922; predicted: probable fructokinase-4 (*Beta vulgaris* subsp. *vulgaris)*	forward: CAATGGAGGAAG CCAAAAAGG reverse: TAAATCCATCCAA GCTTCCCTT	65 °C 22 cycles 294 bp
Glucose-6-phosphate dehydrogenase	Bv4_079860_qtuq	XM_010676236/ XM_01067623; predicted: glucose-6-phosphate 1-dehydrogenase 4, chloroplastic, 2 transcript variants (*Beta vulgaris* subsp. *vulgaris)*	forward: ATTAGAGCTGGGA CAGGACT reverse: TCACTTCTCATGA ATAGATGGT	58 °C 27 cycles 317 bp
Hexokinase	Bv9_224680_aote	XM_010667583/ XM_010667584; predicted: hexokinase-1 (LOC104883130), 2 transcript variants (*Beta vulgaris* subsp. *vulgaris)*	forward: AGAGATACCAATG CTTTCCCT reverse: AGAAGCTCTTTCA ATGTGTGC	65 °C 27 cycles 240 bp
Phospho-fructokinase	Bv9_212010_mhum	XM_010691839; predicted: ATP-dependent 6-phospho-fructokinase 3 (*Beta vulgaris* subsp. *vulgaris)*	forward: TCAAGCAGCAGG AGTGGGT reverse: CACATCCTGTCAG TTATCACA	58 °C 27 cycles 214 bp
Phospho-gluco-isomerase	Bv1_007880_snqy	XM_010677045; predicted: glucose-6-phosphate isomerase 1, chloroplastic (*Beta vulgaris* subsp. *vulgaris)*	forward: GGGCTATATGCCT CACTAGT reverse: AGGAGAACCACA GTTGCCTT	58 °C 24 cycles 273 bp
Phospho-gluco-mutase	Bv6_144320_unms	XM_010683613; predicted: phosphoglucomutase, cytoplasmic (*Beta vulgaris* subsp. *vulgaris)*	forward: CAGAAGGTGAAC CACCTGAA reverse: CTGAACATTGTCC AGCATCC	62 °C 25 cycles 288 bp
Sucrose synthase	Bv7_163460_jmqz	XM_010686041; predicted: sucrose synthase (SBSS1), (*Beta vulgaris* subsp. *vulgaris)*	forward: TGTCAAGTGCAGA GAGGATC reverse: GTTGGCCAGATCA CGGAAC	62 °C 24 cycles 217 bp
UDP-glucose-pyrophospho-rylase	Bv4_096640_ydmd	XM_010696669; predicted: UTP-glucose-1-phosphate uridylyltransferase (LOC104907700), (*Beta vulgaris* subsp. *vulgaris)*	forward: GAAAGGTGACAG TCAATGCC reverse: TGCCAGTTCTGCT AAAGTTTG	62 °C 24 cycles 313 bp
Vacuolar invertase	Bv3_056080_iafj	XM_010673724; predicted: beta-fructofuranosidase, soluble isoenzyme I (LOC104888690)	forward: TCGGCTTATGGGT CGGGTA reverse: TTGCATCATAAGT CACAACCC	62 °C 27 cycles 310 bp

UGPase, PGI, PGM, Ald, PFK, G6PDH, AGPase, and SPS – two or more isoforms each are encoded in the sugar beet genome according to the annotation/prediction of the current gene models (Table 2). With a few exceptions (see Table 2), probes for the respective genes were available on the Agilent array employed for this study.

The absolute signal intensities and the patterns of developmental regulation differed strongly between the individual isoforms of the carbohydrate-metabolic enzymes (see heat map in Table 4). Therefore, overall signal intensities were calculated for the genes encoding each group of isoenzymes (Fig. 2 and Fig. 3) to facilitate the comparison of the developmental patterns of gene expression with the patterns of developmental regulation previously observed for in vitro enzyme activities as described by Jammer & al. (2020; see Table 1). Transcript levels for vacuolar and cell wall-bound invertases were strongly down-regulated from 20 das onwards (Fig. 2), while overall transcript levels for genes encoding SuSys (Fig. 2), FKs (Fig. 2), PGIs (Fig. 2), G6PDHs (Fig. 3), UGPases (Fig. 3), and PFKs (Fig. 3) were up-regulated as storage root development progressed. Transcript levels for aldolases (Fig. 3) also increased, but in a less pronounced fashion and with transient peaks at 30 or 40 das. For the genes encoding cytoplasmic invertases (Fig. 2), PGMs (Fig. 2), and HXKs (Fig. 2), transient increases in transcript levels could be observed, the maxima of which could be found between 20 and 40 das. AGPase (Fig. 3) and SPS transcript levels (Fig. 3) also

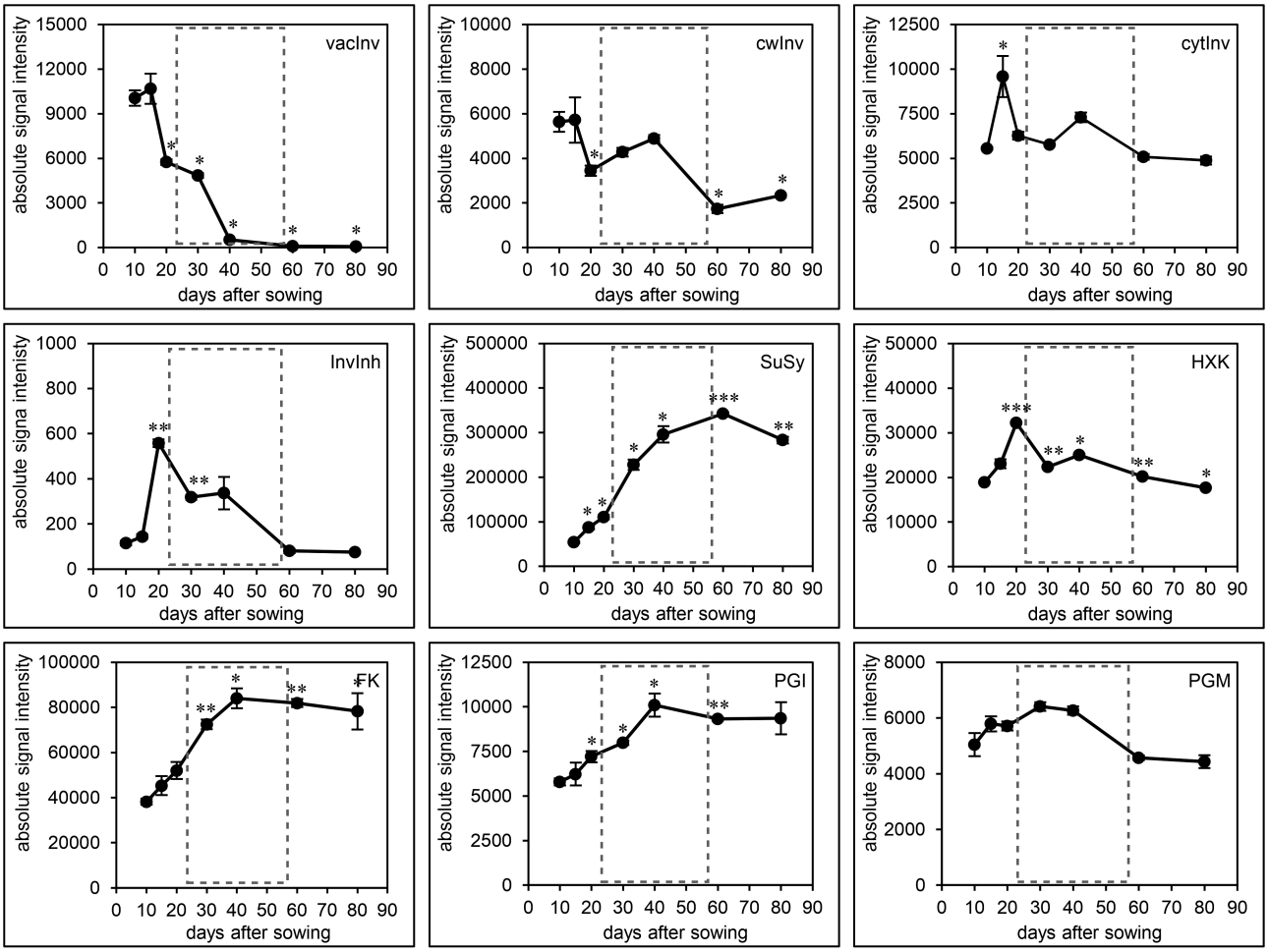

Fig. 2. Microarray expression analysis for genes encoding carbohydrate-metabolic enzymes and related proteins in developing sugar beet taproots over a period of 80 days after sowing. The transition stage from primary root growth to secondary thickening and sucrose storage is marked by the grey box. Overall transcript levels for each enzyme from microarray analysis (total of absolute signal intensities for all isoforms) are shown as means of two technical replicates ± standard deviation (two independent hybridizations each for two independent RNA extracts per sampling time point). Asterisks indicate statistical significance (Welch's t-test; * = $p < 0.05$; ** = $p < 0.01$; *** = $p < 0.001$). cwInv = cell wall invertase; cytInv = cytoplasmic invertase; FK = fructokinase; HXK = hexokinase; InvInh = putative invertase inhibitor protein; PGI = phosphoglucoisomerase; PGM = phosphoglucomutase; SuSy = sucrose synthase; vacInv = vacuolar invertase.

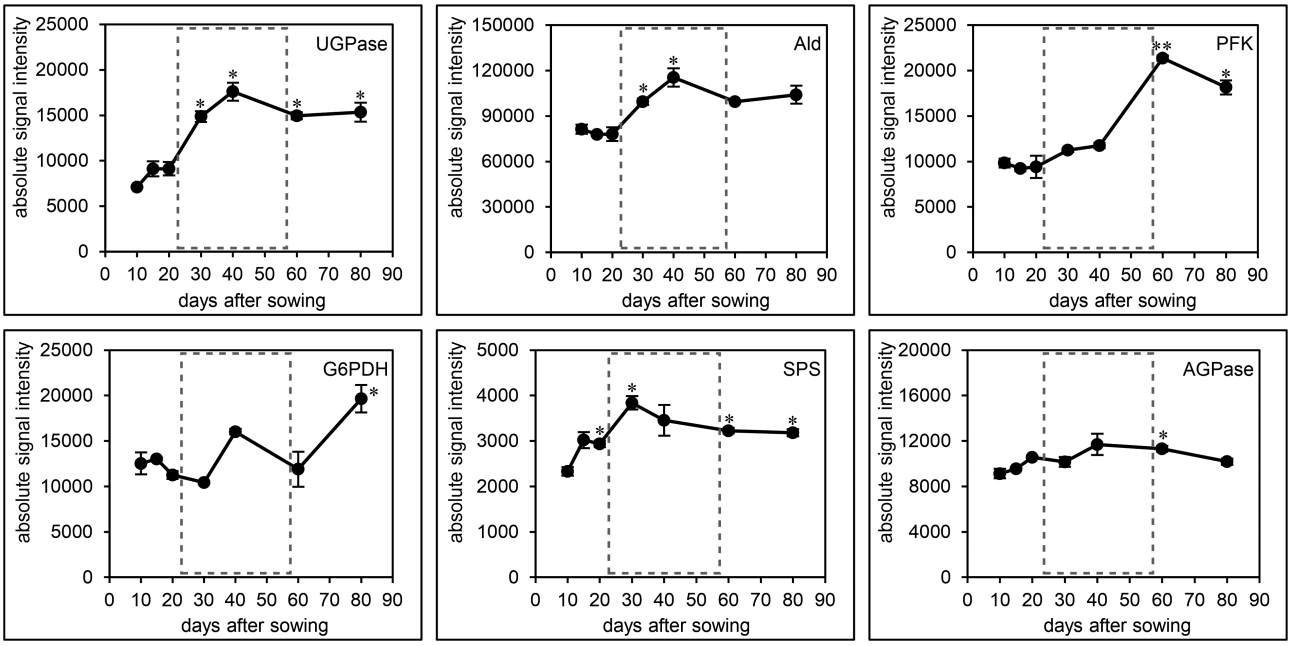

Fig. 3. Microarray expression analysis for genes encoding carbohydrate-metabolic enzymes and related proteins in developing sugar beet taproots over a period of 80 days after sowing. The transition stage from primary root growth to secondary thickening and sucrose storage is marked by the grey box. Overall transcript levels for each enzyme from microarray analysis (total of absolute signal intensities for all isoforms) are shown as means of two technical replicates ± standard deviation (two independent hybridizations each for two independent RNA extracts per sampling time point). Asterisks indicate statistical significance (Welch's t-test; * = $p < 0.05$; ** = $p < 0.01$; *** = $p < 0.001$). AGPase = ADP-glucose pyrophosphorylase; Ald = aldolase; G6PDH = glucose-6-phosphate dehydrogenase; PFK = phosphofructokinase; SPS = sucrose-phosphate synthase; UGPase = UDP-glucose pyrophosphorylase.

showed a very slight increase. In general, the observed changes in transcript levels mostly occurred between 30 and 60 das.

3.2. Semi-qRT PCR validation of microarray data

The microarray data were validated by semi-qRT PCR for selected transcripts (see Table 3), using the expression levels at 10 das as a common reference. The curve shapes of the graphs obtained from the semi-qRT PCR data were very similar to those obtained from the microarray data (for a direct comparison of the microarray and semi-qRT PCR graphs, see Fig. 4 and Fig. 5).

4. Discussion

In systems biology approaches, physiological parameters such as enzyme activities are often excluded in favor of gene expression analysis. However, expression analysis can be misleading when not supplemented with physiological data, as enzyme activities in planta are a product of transcriptional, post-transcriptional, and post-translational regulation. Consequently, there frequently is no direct correlation between steady-state mRNA levels and enzyme activities (e.g., Keurentjes & Sulpice 2009, Bonfig & al. 2010, Stitt & al. 2010, Dai & al. 2011). For this reason, our previous study of early-stage sugar beet taproot development (Jammer & al. 2020) focused on direct measurements of physiological parameters in the first place. Nonetheless, we were interested in the regulatory mechanisms behind the physiological changes we observed, such as in the extent of direct transcriptional regulation of enzyme activities. In the present work, we thus complemented our previous dataset with steady-state expression data for the genes encoding carbohydrate-metabolic enzymes.

The gene expression data were obtained from microarray analysis and subsequently validated for selected genes by semi-qRT PCR. The results obtained for these genes were very similar between the two methods, as can be seen from the direct comparison of the microarray and semi-qRT PCR graphs in Fig. 4 and Fig. 5. However, due to the lower sensitivity and the lower level of precision of the semi-qRT PCR method, the dynamics in the developmental changes of expression detected by this method were less pronounced in comparison to those detected by the microarray. This was particularly the case for the genes that showed very high levels of regulation (e.g., *Bv3_056080_iafj*, encoding a vacInv; see Fig. 4A).

Table 4. Gene expression (microarray) for genes encoding carbohydrate-metabolic enzymes in developing sugar beet storage roots up to 80 days after sowing (das). Relative changes in gene expression (log2 ratio) normalized to 10 das values are shown as mean values of two array hybridizations. Asterisks indicate statistically significant differences from 10 das expression levels (Welch's t-test; * = p < 0.05; ** = p < 0.01; *** = p < 0.001).

gene product	RefBeet1.2 protein ID	das							expression level (range of absolute signal intensity)
		10	15	20	30	40	60	80	
AGPase	Bv_004380_znjm		*	*	*	*	**	*	4 – 2476
	Bv9_217200_yktd					*			117 – 290
	Bv9_206950_yrsx						*	*	2426 – 3669
	Bv1_007110_kmky				*		*		3239 – 8569
Ald	Bv6_129880_fskg		*		*	***	*	*	793 – 20780
	Bv4_091040_cyuu							*	1488 – 8155
	Bv9_214690_sjah					*			341 – 500
	Bv7_159930_ugdi					*	*		8820 – 14640
	Bv4_078150_cgxu			*	*	**	*	*	1899 – 4985
	Bv7_160160_nqkh				*		*		44057 – 92220
cwInv	Bv2_034520_mthe				*		*	*	45 – 203
	Bv7_170580_aiyc			**			*		1642 – 5532
	Bv7_159240_owqs								3.2 – 4.5
cytInv	Bv1_016180_pewc			*				*	1052 – 3400
	Bv1_001200_oroi		**			*	**	***	1720 – 4341
	Bv9_214690_sjah					*			341 – 500
	Bv4_080050_ocda			*			**		455 – 824
	Bv_007210_orig		*	*		*	*	***	428 – 1010
FK	Bv2_027840_oqrd					*	*		5752 – 2185
	Bv8_182100_hsoh						**		292 – 405
	Bv6_136290_jzyk						*		367 – 518
	Bv5_120550_omcz								1678 – 2071
	Bv3_066020_xjni					*	*	**	348 – 554
	Bv3_057460_dyyp				*	*	**		29288 – 78334
	Bv7_178860_gedd			*	*	*	*	*	36 – 213
G6PDH	Bv9_206300_yiew				*			**	516 – 1904
	Bv6_150380_hjur								1005 – 1468
	Bv1_011600_gazr								7546 – 17270
	Bv4_079860_qtuq						*		318 – 782
HXK	Bv8_197580_aaut							*	6167 – 11658
	Bv5_124820_xpum							*	2547 – 5050
	Bv9_224680_aote								735 – 949
	Bv4_073320_tcog		**			*	*	*	2222 – 4869
	Bv9_224670_aurc			**				*	2577 – 15287
InvInh	Bv6_139440_ueqi			*	*	*		*	75 – 558
PFK	Bv6_153060_mqdn						*	*	3.9 – 9.5
	Bv2_046600_nsyu								75 – 183
	Bv6_138960_rsmr						*		787 – 1214
	Bv8_185430_exsc				*	*			3236 – 5340
	Bv8_197870_dtpx					*	*		3607 – 12238
	Bv9_212010_mhum				*	**	*	**	462 – 4206
PGI	Bv5_108180_qtni						*	*	1822 – 3173
	Bv1_007880_snqy				*		*		3965 – 6923
PGM	Bv3_066000_riyk			*	*	*			1105 – 1903
	Bv6_144320_unms								2685 – 5163
SPS	Bv2_030670_mgoq			*		*	*		242 – 1173
	Bv8_193450_doak			*	*		**	*	1791 – 2937
SuSy	Bv4_084720_myet		*	**	*		*		659 – 1578
	Bv8_190960_nnjy		*	*	**	**	*	**	49987 – 262940
	Bv7_163460_jmqz			*	**	**	**	**	3321 – 103446
UGPase	Bv2_045760_wmnk			*	*		*	*	387 – 657
	Bv4_096640_ydmd				*	*	*	*	7094 – 17602
vacInv	Bv5_097930_juac					**	*	**	3.4 – 5448
	Bv3_056080_iafj			*		***	**	**	58 – 5656

Color legend	-11	-10	-9	-8	-7	-6	-5	-4	-3	-2	-1	0	1	2	3	4	5

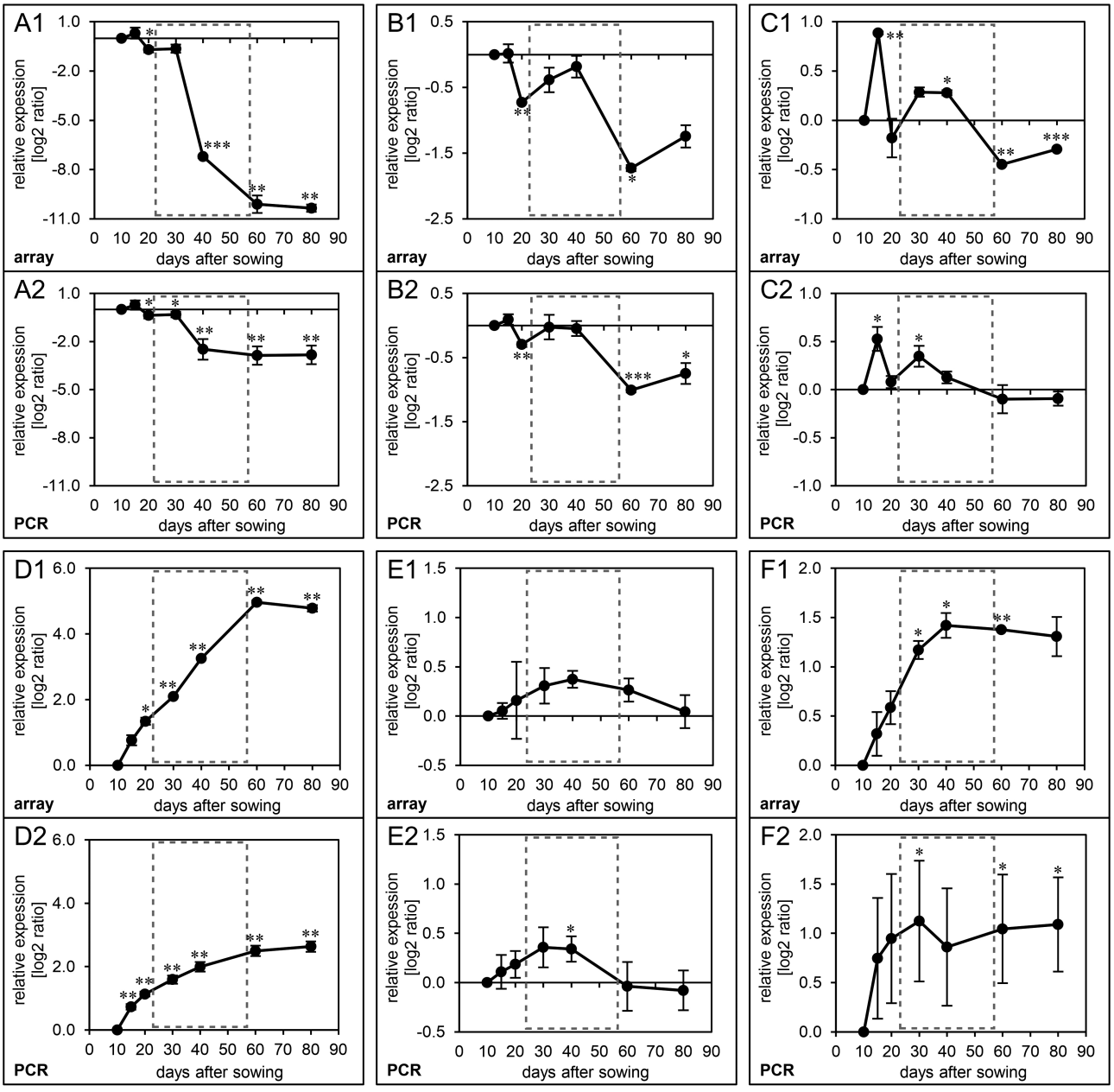

Fig. 4. Semi-qRT PCR validation of microarray expression data for genes encoding carbohydrate-metabolic enzymes in developing sugar beet taproots over a period of 80 days after sowing. The transition stage from primary root growth to secondary thickening and sucrose storage is marked by the grey box. Array data (panels A1 – F1) and semi-qRT PCR data (panels A2 – F2) for the selected genes are shown side by side. Relative gene expression (log2 values) was calculated for each gene using 10 das values as a common reference. Values are shown as means of two technical replicates ± standard deviation (two independent array hybridizations and PCRs each for two independent RNA extracts per sampling time point). Asterisks indicate statistical significance (Welch's t-test; * = $p < 0.05$; ** = $p < 0.01$; *** = $p < 0.001$). [A1/A2] *Bv3_056080_iafj* (encodes a vacuolar invertase). – [B1/B2] *Bv7_170580_aiyc* (encodes a cell wall invertase). – [C1/C2] *Bv1_001200_oroi* (encodes a cytoplasmic invertase). – [D1/D2] *Bv7_163460_jmqz* (encodes a sucrose synthase). – [E1/E2] *Bv9_224680_aote* (encodes a hexokinase). – [F1/F2] *Bv3_057460_dyyp* (encodes a fructokinase).

The changes in transcript levels observed in our study predominantly occurred between 20 and 60 das, and thus, coincided with the developmental stage of the roots previously defined as the "transition stage" (Jammer & al. 2020). At this stage, at around 30 to 60 das in our experiments, the young sugar beet roots undergo a transition from primary root growth to simultaneous secondary thickening and sucrose storage. This transition is accompanied by a characteristic switch in the roots' physiological

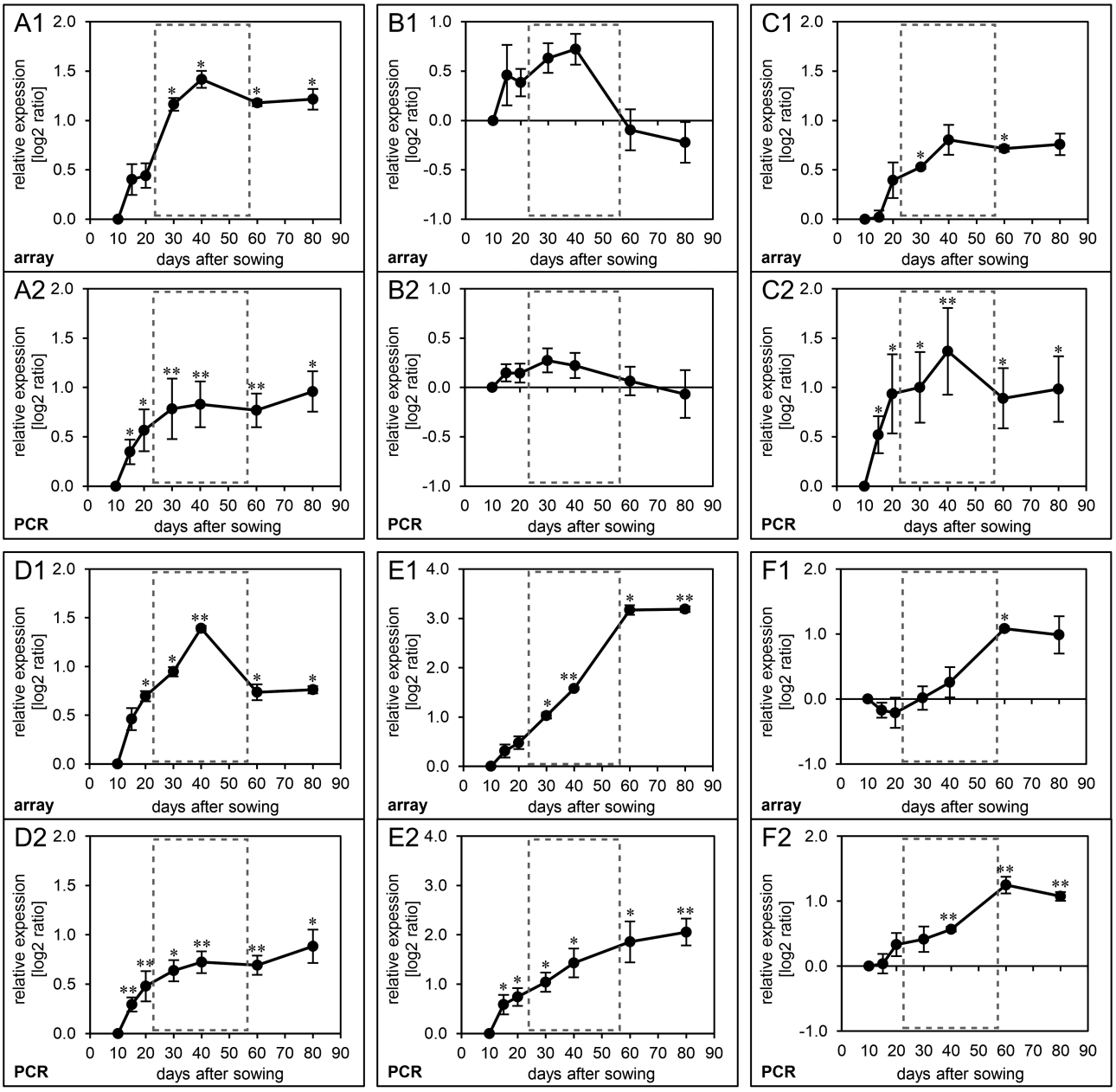

Fig. 5. Semi-qRT PCR validation of microarray expression data for genes encoding carbohydrate-metabolic enzymes in developing sugar beet taproots over a period of 80 days after sowing. The transition stage from primary root growth to secondary thickening and sucrose storage is marked by the grey box. Array data (panels A1 – F1) and semi-qRT PCR data (panels A2 – F2) for the selected genes are shown side by side. Relative gene expression (log2 values) was calculated for each gene using 10 das values as a common reference. Values are shown as means of two technical replicates ± standard deviation (two independent array hybridizations and PCRs each for two independent RNA extracts per sampling time point). Asterisks indicate statistical significance (Welch's t-test; * = $p < 0.05$; ** = $p < 0.01$; *** = $p < 0.001$). [A1/A2] *Bv4_096640_ydmd* (encodes a UDP-glucose pyrophosphorylase). – [B1/B2] *Bv6_144320_unms* (encodes a phosphoglucomutase). – [C1/C2] *Bv1_007880_snqy* (encodes a phosphoglucoisomerase). – [D1/D2] *Bv4_078150_cgxu* (encodes an aldolase). – [E1/E2] *Bv9_224680_aote* (encodes a phosphofructokinase). – [F1/F2] *Bv4_079860_qtuq* (encodes a glucose-6-phosphate dehydrogenase).

signature that becomes evident by pronounced changes in carbohydrate-metabolic enzyme activities, soluble carbohydrate content, and hexose-phosphate levels (see summary in Table 1). A clear developmental shift on the transcriptional level in developing sugar beet taproots has also been reported by Trebbi & McGrath (2009). In their study on greenhouse-grown sugar beet, this shift occurred at 4 to 6 weeks after emergence, which corresponds to approximately 33 to 47 das. According to the in-

formation given on beet fresh weight and sucrose accumulation rates, plant development progressed faster in these experiments than in our experiments, which means that the timing of the developmental shift in gene expression observed by Trebbi & McGrath (2009) corresponds to the transition stage we described in our previous study (Jammer & al. 2020) and in the present study. However, Trebbi & McGrath (2009) did not observe any regulation in transcript levels for genes encoding carbohydrate-metabolic enzymes. This finding can most likely be ascribed to the low sensitivity of the methods used by the authors, and to the fact that the sugar beet genome had not yet been sequenced in 2009, limiting the number of annotated transcripts. In a more recent transcriptomic profiling study on developing sugar beet taproots by Zhang & al. (2017), developmental regulation of several genes encoding invertases, sucrose synthases, and sucrose-phosphate synthases could be observed. However, there is very limited comparability between the data of Zhang & al. (2017) and our data, as the youngest developmental stage analyzed by Zhang & al. (2017) corresponds to the latest developmental stage analyzed in our study, and therefore, to the secondary growth and sucrose storage stage. Our data are still in agreement with the data of Zhang & al. (2017) in two aspects: Firstly, we found that the transcript levels for genes encoding vacInvs and cwInvs strongly decreased at the onset of secondary growth and sucrose storage, and Zhang & al. (2017) also reported low invertase transcript levels at all stages investigated in their study. Secondly, we observed a strong increase in transcripts encoding SuSy proteins from the transition stage onwards, and high transcript levels for SuSy-encoding genes were also reported by Zhang & al. (2017).

At the onset of sucrose storage in sugar beet taproots, a rapid reduction in invertase activities, particularly in the vacuoles, is required – and could also be observed in our physiological study (Jammer & al. 2020) – in order to allow the accumulation of large amounts of sucrose. However, a certain amount of the incoming sucrose still needs to be cleaved to obtain the hexose monomers required to release energy through glycolysis and to provide building blocks for complex carbohydrates. This function is taken over by SuSy as the key sucrolytic enzyme in actively growing sink organs (recently reviewed by Stein & Granot 2019, Zierer & al. 2021). A shift from apoplasmic to symplasmic phloem unloading, visible through an inverse developmental regulation of invertases and sucrose synthases, is a commonly observed phenomenon during storage root and tuber development, and appears to be characteristic for the transition from primary growth to storage root/tuber formation (recently reviewed by Zierer & al. 2021). SuSy has also been shown to be an important determinant of sink strength in actively growing sink organs (recently reviewed by Stein & Granot 2019). On the mRNA level, the up-regulation of SuSy-encoding genes at the onset of storage root/tuber development seems to occur in a species-independent manner and has also been described for potato (Ferreira & al. 2010), cassava (Huang & al. 2021, Pan & al. 2021), sweet potato (Tao & al. 2012, Dong & al. 2019), carrot (Sturm & al. 1995, Sturm 1996), and radish (Mitsui & al. 2015, Yu & al. 2016).

For most of the other gene families we investigated, little information is available from other storage root-/tuber-forming species on the developmental regulation during the transition from primary root growth to storage root formation. Some of the gene families that were up-regulated in our present study also showed a trend of up-regulation in developing storage roots/tubers in other species: FK-encoding genes were up-regulated in potato (Ferreira & al. 2010) and sweet potato (Tao & al. 2012); UGPase-encoding genes were up-regulated in potato (Zrenner & al. 1993, Ferreira & al. 2010) and sweet potato (Tao & al. 2012); PGM-encoding genes were up-regulated in potato (Ferreira & al. 2010) and sweet potato (Firon & al. 2013); PFK-encoding genes were up-regulated in sweet potato (Firon & al. 2013) and cassava (Wang & al. 2021).

It needs to be pointed out that we saw a high level of similarity between the developmental patterns of in vitro enzyme activities from our previous study (Jammer & al. 2020) and the transcript levels of the respective genes from our present study. The developmental changes in overall gene expression patterns were in good accordance with the respective enzyme activity patterns for vacInv, cwInv, SuSy, PGI, UGPase, G6PDH, Ald, and PFK. For these enzymes, the activity levels at the early stages of sugar beet taproot development appear to be predominantly regulated on the transcriptional level. This was unexpected, as it is frequently reported that there is a lack of correlation between gene expression levels and enzyme activities (e.g., Bonfig & al. 2010, Dai & al. 2011). For the cases where the in vitro enzyme activity patterns deviated from the gene expression patterns (PGM, cytInv, HXK, FK), post-transcriptional and/or post-translational mechanisms need to be taken into account as regulators of enzyme activities (Keurentjes & al. 2008, Keurentjes & Sulpice 2009, Stitt & al. 2010). For SPS, a slight increase in transcript levels was observed, while activities of this enzyme remained unchanged at very low levels in our physiological study. Similarly, for AGPase, we observed a very slight increase in transcript levels, but enzyme ac-

tivities and transcript levels could not be directly compared, as AGPase activity was below or near the limit of detection in our physiological study.

When combining the data from the analyses of gene expression and enzyme activities, another observation needs to be addressed: the enzyme activities of vacInv and cwInv rapidly declined from 10 das onwards, while the transcript levels from genes encoding the respective proteins only started to decline from 15 das onwards. Godt & Roitsch (2006) also reported that the rapid loss of cwInv activity in developing sugar beet taproots was caused by a strong transcriptional down-regulation. However, in our study and in the study of Godt & Roitsch (2006), the decrease in invertase enzyme activities preceded the decrease in transcript levels. As the glycosylated vacInv and cwInv proteins are highly stable, a rapid down-regulation of invertase activities cannot be achieved by transcriptional regulation alone, but is supported on the post-translational level by the action of proteinaceous invertase inhibitors (Rausch & Greiner 2004, Castrillón-Arbeláez & Délano-Frier 2011). The involvement of invertase inhibitor proteins in the rapid regulation of invertases by repression or de-repression during developmental processes or in other contexts has been shown in many studies (e.g., Bonfig & al. 2010, Katz & al. 2011, Albacete & al. 2014, Qin & al. 2016, Su & al. 2016, Tang & al. 2017, Shen & al. 2019, Su & al. 2020). In our microarray analysis, the transcript abundance for a gene encoding a putative invertase inhibitor protein was observed to be transiently up-regulated at 20 to 40 das (*Bv6_139440_ueqi*, Fig. 2). An up-regulation of a gene encoding an invertase inhibitor-like protein was also observed by Tao & al. (2012) in developing tuberous roots of sweet potato. Therefore, we assume that invertase inhibitor proteins may indeed be involved in the down-regulation of invertase activities during the metabolic transition from primary root growth to taproot development. This finding shows the work of Godt & Roitsch (2006) in a new light: In their study, the authors ruled out the involvement of such invertase inhibitors in the regulation of cwInv activity in developing taproots. This conclusion was based on invertase activity assays with mixed extracts, where extracts from 78-day-old taproots did not show any negative influence on invertase activities in extracts from 10-day-old taproots. Our present data suggest that this observation might have been a consequence of a transient expression of the invertase inhibitors at the transition stage, i.e., that the inhibitor proteins were no longer present at 78 das. However, additional gene and protein expression studies, as well as physiological studies will be required to test the hypothesis of an inhibitor-mediated post-translational regulation of invertase activities in young sugar beet taproots during the transition stage.

Furthermore, a general trend of up-regulation in HXK transcripts could be observed during the transition stage (Fig. 2), in the absence of increased HXK enzyme activity (Jammer & al. 2020). A dual role of HXK has been described for photosynthetically active tissues, where HXK1 acts as a negative regulator of photosynthesis when glucose is abundant, while the exact mechanism of the HXK-mediated growth-regulatory function is still relatively unclear (reviewed by Granot & al. 2014). In addition, Kushwah & Laxmi (2017) recently suggested a potential role of HXK1 in the integration of glucose and hormonal signals for root length control. HXK has also been reported to play a role in the transcriptional regulation of cwInv and SuSy in developing grape berries (Wang & al. 2014, Zhang & al. 2014). Thus, we assume that HXK might not only act as a hexose-phosphorylating enzyme but also as a glucose sensor in developing sugar beet taproots. This idea is also supported by the fact that three of the HXK genes that were up-regulated transiently at the transition stage (*Bv8_197580_aaut*, *Bv9_224670_aurc*, *Bv9_224680_aote*) have been predicted to encode HXK1 proteins. In summary, our observations concerning deviating patterns in HXK enzyme activity and transcript levels suggest that it may be worthwhile to further look into the role of HXKs in developing sugar beet taproots during the stage transition from primary root development to secondary growth and sucrose storage.

Taken together, the findings from our two studies (Jammer & al. 2020 and the present study) emphasize the benefits that arise from the combination of analyses on different levels: cell physiological assays and gene expression analyses performed on the same material within a holistic phenomics approach (Grosskinsky & al. 2015, 2017) lead to the identification of potential regulatory mechanisms that would have remained elusive otherwise (Pandey et al. 2021). Therefore, it will be important in future studies to include additional levels, such as non-targeted transcriptomics and metabolomics, additional cell- and eco-physiological studies, in-situ techniques to assess spatio-temporal dynamics of transcripts and enzyme activities, and functional research employing genetically modified sugar beet plants. Only when taking into account a broad range of aspects, the determinants for taproot formation and sucrose accumulation, and thus, the key regulators for the development of the sucrose-storing taproot, may eventually be identified. In conclusion, our data highlighted once more the importance of including the earliest stages of taproot development in future studies when aiming to identify

the determinants for ultimate sink strength, which defines the potential for total sucrose accumulation in mature beets.

Acknowledgements

The work of our technical assistants Anna Luidold, Peter Krbez, Tanja Mayer, and Ursula Janschek is gratefully acknowledged. The authors would also like to thank Prof. Peter M. Roth for his support with statistical data analysis. The presented research was funded by KWS SAAT SE & Co. KGaA (Einbeck, Germany) and supported by the Ministry of Education, Youth and Sports of the Czech Republic within the National Sustainability Program I (NPU I; grant number LO1415) and The Czech Science Foundation (GA CR; grant number 15-17367S).

References

Albacete A., Cantero-Navarro E., Balibrea M. E., Grosskinsky D. K., de la Cruz González M., Martínez-Andújar C., Smigocki A. C., Roitsch T. & Pérez-Alfocea F. 2014. Hormonal and metabolic regulation of tomato fruit sink activity and yield under salinity. – Journal of Experimental Botany 65: 6081–6095.

Artschwager E. 1926. Anatomy of the vegetative organs of the sugar beet. – Journal of Agricultural Research 33: 143–176.

Artschwager E. 1930. A study of the structure of sugar beets in relation to sugar content and type. – Journal of Agricultural Research 40: 867–915.

Bellin D., Werber M., Theis T., Schulz B., Weisshaar B. & Schneider K. 2002. EST sequencing, annotation and macroarray transcriptome analysis identify preferentially root-expressed genes in sugar beet. – Plant Biology 4: 700–710.

Bellin D., Schulz B., Soerensen T. R., Salamini F. & Schneider K. 2007. Transcript profiles at different growth stages and tap-root zones identify correlated developmental and metabolic pathways of sugar beet. – Journal of Experimental Botany 58: 699–715.

Bergen P. 1967. Dry matter of the petiole as an index for the selection of sugar beet plants. – Journal of the American Society of Sugar Beet Technologists 14: 396–399.

Bonfig K. B., Gabler A., Simon U. K., Luschin-Ebengreuth N., Hatz M., Berger S., Muhammad N., Zeier J., Sinha A. K. & Roitsch T. 2010. Post-translational derepression of invertase activity in source leaves via down-regulation of invertase inhibitor expression is part of the plant defense response. – Molecular Plant 3: 1037–1048.

Bosemark N. O. 2006. Genetics and breeding. – In: Draycott A. P. (ed.), Sugar beet, p. 50–88. – Blackwell Publishing; Oxford, United Kingdom.

Castrillón-Arbeláez P. A. & Délano-Frier J. P. 2011. The sweet side of inhibition: invertase inhibitors and their importance in plant development and stress responses. – Current Enzyme Inhibition 7: 169–177.

Dai N., Cohen S., Portnoy V., Tzuri G., Harel-Beja R., Pompan-Lotan M., Carmi N., Zhang G., Diber A., Pollock S., Karchi H., Yeselson Y., Petreikov M., Shen S., Sahar U., Hovav R., Lewinsohn E., Tadmor Y., Granot D., Ophir R., Sherman A., Fei Z., Giovannoni J., Burger Y., Katzir N. & Schaffer A. A. 2011. Metabolism of soluble sugars in developing melon fruit: a global transcriptional view of the metabolic transition to sucrose accumulation. – Plant Molecular Biology 76: 1–18.

Doney D. L. 1979. Seedling physiology and sugarbeet yield. – Journal of the American Society of Sugar Beet Technologists 20: 399–418.

Doney D. L., Wyse R. E. & Theurer J. C. 1981. The relationship between cell size, yield, and sucrose concentration of the sugar beet root. – Canadian Journal of Plant Science 61: 447–453.

Dong T., Zhu M., Yu J., Han R., Tang C., Xu T., Liu J. & Li Z. 2019. RNA-Seq and iTRAQ reveal multiple pathways involved in storage root formation and development in sweet potato (*Ipomoea batatas* L.). – BMC Plant Biology 19(1): 136.

Elliott M. C. & Weston G.D. 1993. Biology and physiology of the sugar-beet plant. – In: Cooke D. A. & Scott R. K. (eds.), The sugar beet crop. Science into practice, p. 37-66. – Chapman & Hall; London.

Fasahat P., Aghaeezadeh M., Jabbari L., Sadeghzadeh Hemayati S. & Townson P. 2018. Sucrose accumulation in sugar beet: From fodder beet selection to genomic selection. – Sugar Tech 20: 635–644.

Fasahat P., Aghaeezadeh M., Hosseinpour M. & Sadeghzadeh Hemayati S. 2021. Correlation between root weight and sugar content; do we have to continue traditional hypothesis? – Plant Physiology Reports 26: 188–191.

Ferreira S. J., Senning M., Sonnewald S., Kessling P.-M., Goldstein R. & Sonnewald U. 2010. Comparative transcriptome analysis coupled to X-ray CT reveals sucrose supply and growth velocity as major determinants of potato tuber starch biosynthesis. – BMC Genomics 11: 93.

Firon N., LaBonte D., Villordon A., Kfir Y., Solis J., Lapis E., Perlman T. S., Doron-Faigenboim A., Hetzroni A., Althan L. & Adani Nadir L. 2013. Transcriptional profiling of sweetpotato (*Ipomoea batatas*) roots indicates down-regulation of lignin biosynthesis and up-regulation of starch biosynthesis at an early stage of storage root formation. – BMC Genomics 14: 460.

Getz H.-P. 2000. Sucrose accumulation and synthesis in sugar beets. – Developments in Crop Science 26: 55–77.

Giaquinta R. 1979. Sucrose translocation and storage in the sugar beet. – Plant Physiology 63: 828–832.

Godt D. & Roitsch T. 2006. The developmental and organ specific expression of sucrose cleaving enzymes in sugar beet suggests a transition between apoplasmic and symplasmic phloem unloading in the tap roots. – Plant Physiology and Biochemistry 44: 656–665.

Granot D., Kelly G., Stein O. & David-Schwartz R. 2014. Substantial roles of hexokinase and fructokinase in the effects of sugars on plant physiology and development. – Journal of Experimental Botany 65: 809–819.

Grosskinsky D. K., Svensgaard J., Christensen S. & Roitsch T. 2015. Plant phenomics and the need for physiological phenotyping across scales to narrow the genotype-to-phenotype knowledge gap. Journal of Experimental Botany 66: 5429–5440.

Grosskinsky D.K., Syaifullah S. J. & Roitsch T. 2017. Integration of multi-omics techniques and physiological phenotyping within a holistic phenomics approach to study senescence in model and crop plants. Journal of Experimental Botany 69: 825–844.

Herwig R., Schulz B., Weisshaar B., Hennig S., Steinfath M., Drungowski M., Stahl D., Wruck W., Menze A., O'Brien J., Lehrach H. & Radelof U. 2002. Construction of a 'unigene' cDNA clone set by oligonucleotide fingerprinting allows access to 25 000 potential sugar beet genes. – Plant Journal 32: 845–857.

Hoffmann C. M., Kenter C. & Bloch D. 2005. Marc concentration of sugar beet (*Beta vulgaris* L) in relation to sucrose storage. – Journal of the Science of Food and Agriculture 85: 459–465.

Huang T., Luo X., Fan Z., Yang Y. & Wan W. 2021. Genome-wide identification and analysis of the sucrose synthase gene family in cassava (*Manihot esculenta* Crantz). – Gene 769: 145191.

Jammer A., Albacete A., Schulz B., Koch W., Weltmeier F., van der Graaff, Eric, Pfeifhofer H. W. & Roitsch T. G. 2020. Early-stage sugar beet taproot development is characterized by three distinct physiological phases. – Plant Direct 4: e00221.

Katz E., Boo K. H., Kim H.Y., Eigenheer R. A., Phinney B. S., Shulaev V., Negre-Zakharov F., Sadka A. & Blumwald E. 2011. Label-free shotgun proteomics and metabolite analysis reveal a significant metabolic shift during citrus fruit development. – Journal of Experimental Botany 62: 5367–5384.

Keurentjes J. J. B. & Sulpice R. 2009. The role of natural variation in dissecting genetic regulation of primary metabolism. – Plant Signaling & Behavior 4: 244–246.

Keurentjes J. J. B., Sulpice R., Gibon Y., Steinhauser M.-C., Fu J., Koornneef M., Stitt M. & Vreugdenhil D. 2008. Integrative analyses of genetic variation in enzyme activities of primary carbohydrate metabolism reveal distinct modes of regulation in *Arabidopsis thaliana*. – Genome Biology 9: R129.

Krumbiegel A. 1998. Morphology and anatomy in annual taxa of *Beta vulgaris* s.l. (*Chenopodiaceae*). – Nordic Journal of Botany 18: 159–167.

Kushwah S. & Laxmi A. 2017. The interaction between glucose and cytokinin signaling in controlling *Arabidopsis thaliana* seedling root growth and development. – Plant Signaling & Behavior 12: e1312241.

Leigh R. A., Ap Rees T., Fuller W. A. & Banfield J. 1979. The location of acid invertase activity and sucrose in the vacuoles of storage roots of beetroot (*Beta vulgaris*). – Biochemical Journal. 178: 539–547.

Li J., Wu L., Foster R. & Ruan Y.-L. 2017. Molecular regulation of sucrose catabolism and sugar transport for development, defence and phloem function. – Journal of Integrative Plant Biology 59: 322–335.

Milford G. F. J. 2006. Plant structure and crop physiology. – In: Draycott A. P. (ed.), Sugar beet, p. 30–49. – Blackwell Publishing; Oxford, United Kingdom.

Mitsui Y., Shimomura M., Komatsu K., Namiki N., Shibata-Hatta M., Imai M., Katayose Y., Mukai Y., Kanamori H., Kurita K., Kagami T., Wakatsuki A., Ohyanagi H., Ikawa H., Minaka N., Nakagawa K., Shiwa Y. & Sasaki T. 2015. The radish genome and comprehensive gene expression profile of tuberous root formation and development. – Scientific Reports 5: 10835.

Oldemeyer R. K. 1975. Introgressive hybridization as a breeding method in *Beta vulgaris*. – Journal of Sugarbeet Research 18: 269–273.

Pack D. A. 1927. Ring density of sugar beets as a character for selection. – American Journal of Botany 14: 238–245.

Pan K., Lu C., Nie P., Hu M., Zhou X., Chen X. & Wang W. 2021. Predominantly symplastic phloem unloading of photosynthates maintains efficient starch accumulation in the cassava storage roots (*Manihot esculenta* Crantz). – BMC Plant Biology 21(1): 318.

Pandey C., Grosskinsky D. K., Westergaard J. C., Jørgensen H. J. L., Svensgaard J., Christensen S., Schulz A. & Roitsch T. 2021. Identification of a bio-signature for barley resistance against *Pyrenophora teres* infection based on physiological, molecular and sensor-based phenotyping. – Plant Science (article in press). https://doi.org/10.1016/j.plantsci.2021.111072

Powers L. 1956. Identification of genetically-superior individuals and the prediction of genetic gains in sugar beet breeding programs. – Journal of the American Society of Sugar Beet Technologists 9: 408–432.

Qin G., Zhu Z., Wang W., Cai J., Chen Y., Li L. & Tian S. 2016. A tomato vacuolar invertase inhibitor mediates sucrose metabolism and influences fruit ripening. – Plant Physiology 172: 1596–1611.

Rausch T. & Greiner S. 2004. Plant protein inhibitors of invertases. – Biochimica et Biophysica Acta - Proteins and Proteomics 1696: 253–261.

Shen A., Ma S., Liu Y., Liao S., Li J., Wu L., Kartika D., Mock H.-P- & Ruan Y.-L. 2019. Cell wall invertase and sugar transporters are differentially activated in tomato styles and ovaries during pollination and fertilization. – Frontiers in Plant Science 10: 506.

Slewinski T. L. & Braun D. M. 2010. Current perspectives on the regulation of whole-plant carbohydrate partitioning. – Plant Science 178: 341–349.

Stein O. & Granot D. 2019. An Overview of Sucrose Synthases in Plants. – Frontiers in Plant Science 10: 95.

Stich B., Piepho H.-P., Schulz B. & Melchinger A. E. 2008. Multi-trait association mapping in sugar beet (*Beta vulgaris* L.). – Theoretical and Applied Genetics 117(6): 947–954.

Stitt M., Sulpice R. & Keurentjes J. 2010. Metabolic networks: how to identify key components in the regulation of metabolism and growth. – Plant Physiology 152: 428–444.

Sturm A. 1996. Molecular characterization and functional analysis of sucrose-cleaving enzymes in carrot (Daucus carota L.). – Journal of Experimental Botany 47: 1187–1192.

Sturm A., Šebková V., Lorenz K., Hardegger M., Lienhard S. & Unger C. 1995. Development- and organ-specific expression of the genes for sucrose synthase and three isoenzymes of acid β-fructofuranosidase in carrot. – Planta 195(4): 601–610.

Su T., Wolf S., Han M., Zhao H., Wei H., Greiner S. & Rausch T. 2016. Reassessment of an *Arabidopsis* cell wall invertase inhibitor AtCIF1 reveals its role in seed germination and early seedling growth. – Plant Molecular Biology 90: 137–155.

Su T., Han M., Min J., Zhou H., Zhang Q., Zhao J. & Fang Y. 2020. Functional characterization of invertase inhibitors PtC/VIF1 and 2 revealed their involvements in the defense response to fungal pathogen in *Populus trichocarpa*. – Frontiers in Plant Science 10: 1654.

Tang X., Su T., Han M., Wei L., Wang W., Yu Z., Xue Y., Wei H., Du Y., Greiner S., Rausch T. & Liu L. 2017. Suppression of extracellular invertase inhibitor gene expression improves seed weight in soybean (*Glycine max*). – Journal of Experimental Botany 68: 469–482.

Tao X., Gu Y.-H., Wang H.-Y., Zheng W., Li X., Zhao C.-W. & Zhang Y.-Z. 2012. Digital gene expression analysis based on integrated de novo transcriptome assembly of sweet potato *Ipomoea batatas* (L.) Lam. – PLoS ONE 7(4): e36234.

Trebbi D. & McGrath J. M. 2009. Functional differentiation of the sugar beet root system as indicator of developmental phase change. – Physiologia Plantarum 135: 84–97.

Wang H., Zhao P., Shen X., Xia Z., Zhou X., Chen X., Lu C. & Wang W. 2021. Genome-wide survey of the phosphofructokinase family in cassava and functional characterization in response to oxygen-deficient stress. – BMC Plant Biology 21(1): 376.

Wang L. & Ruan Y.-L. 2016. Shoot–root carbon allocation, sugar signalling and their coupling with nitrogen uptake and assimilation. – Functional Plant Biology 43: 105–113.

Wang X. Q., Li L. M., Yang P. P. & Gong C. L. 2014. The role of hexokinases from grape berries (*Vitis vinifera* L.) in regulating the expression of cell wall invertase and sucrose synthase genes. – Plant Cell Reports 33: 337–347.

Weltmeier F., Mäser A., Menze A., Hennig S., Schad M., Breuer F., Schulz B., Holtschulte B., Nehls R. & Stahl D. J. 2011. Transcript profiles in sugar beet genotypes uncover timing and strength of defense reactions to *Cercospora beticola* infection. – Molecular Plant-Microbe Interactions 24: 758–772.

Wyse R. E. 1979. Parameters controlling sucrose content and yield of sugarbeet roots. – Journal of the American Society of Sugar Beet Technologists 20: 368–385.

Yu R., Xu L., Zhang W., Wang Y., Luo X., Wang R., Zhu X., Xie Y., Karanja B. & Liu L. 2016. De novo taproot transcriptome sequencing and analysis of major genes involved in sucrose metabolism in radish (*Raphanus sativus* L.). – Frontiers in Plant Science 7: 585.

Zamski E. & Azenkot A. 1981. Sugarbeet vasculature. II. Translocation of assimilates in the supernumerary phloem. – Botanical Gazette 142: 344–346.

Zhang Y., Zhen L., Tan X., Li L. & Wang X. 2014. The involvement of hexokinase in the coordinated regulation of glucose and gibberellin on cell wall invertase and sucrose synthesis in grape berry. – Molecular Biology Reports 41: 7899–7910.

Zhang Y.-F., Li G.-L., Wang X.-F., Sun Y.-Q., Zhang S.-Y. & Amancio S. 2017. Transcriptomic profiling of taproot growth and sucrose accumulation in sugar beet (*Beta vulgaris* L.) at different developmental stages. – PLoS ONE 12: e0175454.

Zierer W., Rüscher D., Sonnewald U. & Sonnewald S. 2021. Tuber and tuberous root development. – Annual Review of Plant Biology 72: 551-580.

Zrenner R., Willmitzer L. & Sonnewald U. 1993. Analysis of the expression of potato uridinediphosphate-glucose pyrophosphorylase and its inhibition by antisense RNA. – Planta 190(2): 247–252.

(Received 19 Oct 2021, accepted 31 Oct 2021)